

Supporting Information:

**Cathodic oxygen–reduction–reaction–mediated active peroxide  
for oxidizing cyclohexanone to  $\epsilon$ –caprolactone**

Long Chen,<sup>a, b</sup> Shanyong Chen\*<sup>a</sup> and Xiaoqing Qiu\*<sup>a, b</sup>

<sup>a</sup>College of Chemistry and Chemical Engineering, Central South University,  
Changsha, Hunan 410083, P. R. China.

<sup>b</sup>Hunan Provincial Key Laboratory of Chemical Power Sources, Central South  
University, Changsha, Hunan 410083, P. R. China

Email: shanyongchen@csu.edu.cn, xq-qiu@csu.edu.cn

**Contents**

**Experiment section: S1-S4**

**Figures: S5-S25**

**Table: S26-27**

**Reference: S28**

## 1. Experiment section

### 1.1. Reagents

Ketjenblack, iron phthalocyanine, dicyandiamide,  $\epsilon$ -caprolactone, cyclohexanone, cyclobutanone, cyclopentanone, 4-methylcyclohexanone were purchased from Shanghai Aladdin Bio-Chem Technology Co., Ltd. N, N-dimethylformamide, sulfuric acid, and nitric acid were purchased from Sinopharm Chemical Reagent Company. Nafion solution (5 wt.%) was purchased from Alfa Aesar (China). Methanol and 1, 4-benzoquinone were purchased from General-Reagents. All chemicals were directly used without further purification.

### 1.2. Synthesis of materials

*Synthesis of O@C.* Firstly, Ketjenblack (300 mg) was placed in a mixture of sulfuric acid (25 mL) and nitric acid (75 mL), and was treated at 80 °C for 12 h. After cooling to room temperature, perform vacuum filtration and washing with deionized water until the filtrate becomes neutral. The obtained powder was dried under vacuum conditions to gain the product, named O@C.

*Synthesis of Fe<sub>1</sub>NC.* Iron phthalocyanine (30 mg), Ketjenblack (200 mg), and dicyandiamide (0.6 g) were dispersed in N, N-dimethylformamide and stirred at room temperature for 6 h. Subsequently, through rotary evaporation and drying, the obtained powder was heated at a rate of 3 °C min<sup>-1</sup> in a N<sub>2</sub> atmosphere to 850 °C for 2 h. Ultimately, the product was collected via grinding and was labeled as Fe<sub>1</sub>NC.

### 1.3. Characterizations

The morphologies and microstructures of the samples were observed via field emission scanning electron microscopy (FE-SEM, JSM-7610F). X-ray photoelectron spectroscopy (XPS) were acquired on Thermo ESCALAB (250Xi, USA) to study the

chemical states of elements. Raman spectra were recorded on the Laser Micro-Raman Spectrometer (Renishaw InVia, UK).

The liquid nuclear magnetic resonance spectra (NMR) were recorded on a Bruker Avance II 500 MHz in deuterium oxide (D<sub>2</sub>O). The <sup>1</sup>H NMR spectra were obtained using a pre-saturation method for water suppression. Typically, 500 μL of collected catholyte was mixed with 100 μL of internal standard solution (dimethyl sulfoxide in D<sub>2</sub>O). ε-caprolactone production was further verified by GC-MS (GCMS-QP2010ULTRA, Shimadzu Japan). The GC-MS spectral features were determined by comparing the mass fragmentation patterns with those of the National Institute of Standards and Technology library.

#### 1.4. Electrochemical oxygen reduction reaction measurements

All electrochemical ORR experiments were performed on the electrochemical workstation (CHI760E, CH Instrument) with the three-electrode system. The graphite rod and the Ag/AgCl electrode are used as the counter electrode and the reference electrode, respectively. The working electrode is the catalyst-loaded rotating ring-disk electrode (RRDE, 6.5 mm inner diameter and 8.5 mm outer diameter). 0.1 M KOH solution is used as the electrolyte. Before the test, RRDE was mechanically polished with Al<sub>2</sub>O<sub>3</sub> slurry to obtain a mirror-like surface. The catalyst ink was prepared by dispersing 4.0 mg electrocatalyst in 780 μL of ethanol, 200 μL deionized water and 20 μL of Nafion solution (5 wt.%), followed by sonication for 1 h. Subsequently, 25 μL of the as-obtained ink was dripped onto the cleaned RRDE and naturally dried.

The electrochemical measurements were performed in O<sub>2</sub>-saturated 0.1 M KOH solution under room temperature. Prior to the ORR tests, the activation process was carried out by scanning cycle voltammetry (CV) for 20 cycles at a scan rate of 50 mV s<sup>-1</sup> until stable CV curves were obtained. The Linear sweep voltammetry (LSV) curves were conducted at 1600 rpm with the scan rate of 10 mV s<sup>-1</sup>. The Pt ring electrode was maintained at 1.2 V (vs. RHE) to detect the generated H<sub>2</sub>O<sub>2</sub>. And the Pt ring was electrochemically cleaned using scanning CV curves for 20 cycles with sweep rate of 0.5 V s<sup>-1</sup> in potential range from 1.1 to 0.05 V vs. RHE prior to LSV test.

All the potentials in electrochemical test were corrected to the reversible hydrogen electrode (RHE) using the formulas as follows:

$$E_{\text{RHE}} = E_{\text{Ag/AgCl}} + 0.197 + 0.059\text{pH} \quad (1)$$

The transfer electron number ( $n$ ) and  $\text{H}_2\text{O}_2$  selectivity were calculated as equation (2) and (3):

$$n = 4 \frac{I_d}{I_d + \frac{I_r}{N}} \quad (2)$$

$$\text{H}_2\text{O}_2\% = 200 \frac{\frac{I_r}{N}}{I_d + \frac{I_r}{N}} \quad (3)$$

Where  $I_d$  is the disk current,  $I_r$  is the ring current, and  $N$  is the current collection efficiency of the Pt ring (0.37).

### 1.5. Electro-thermochemical cascade catalysis tests

The electro-thermochemical cascade catalysis tests were exemplified by the substrate of cyclohexanone. Electro-thermochemical cascade reaction was conducted on a three-electrode system of H-type cell. The Pt sheet electrode and the Ag/AgCl electrode are used as the counter electrode and the reference electrode, respectively. The working electrode is the catalyst-loaded carbon paper ( $1 \text{ mg cm}^{-2}$ ,  $1 \times 1 \text{ cm}^2$ ).

During the measurement process,  $\text{O}_2$  was injected into the cathode, while the electrolyte was composed of cyclohexanone and 0.1 M KOH. The chronoamperometry measurement was employed to increase the potential stepwise from 0.4 to 0 V vs RHE. The duration of the test was 1 h and a certain volume of cathode electrolyte was taken at the end of the test for quantitative testing.

### 1.6. Kinetic reaction order test

In the in-situ ORR-mediated electro-thermochemical chemical cascade reaction system, the content of  $\text{*OOH}$  is determined by  $\text{H}_2\text{O}_2$ . A mathematical relationship  $\ln[r_{(\varepsilon\text{-CL})}] = \alpha \ln[c_{(\text{H}_2\text{O}_2)}] + A$  between the  $\text{*OOH}$  concentration and the  $\varepsilon$ -caprolactone formation rate is obtained by fitting, thereby determining the reaction order  $\alpha$ . Similarly, by regulating the cyclohexanone substrate concentration, a mathematical

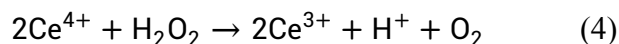
relationship  $\ln[r_{(\epsilon\text{-CL})}] = \beta \ln[c_{(\text{CYC})}] + B$  between the cyclohexanone concentration and the  $\epsilon$ -caprolactone formation rate is obtained, thereby determining the reaction order  $\beta$ .

### 1.7. In-situ Raman measurements

In-situ Raman was measured on inVia Reflex (Renishaw, UK, laser excitation source: 785 nm). The custom-made Teflon reactor with a quartz window was used as the test cell where the Ag/AgCl and Pt wire were employed as the reference and counter electrode, respectively. And the catalyst was loaded on Au as working electrode. In-situ Raman spectra were collected in electrolyte from 0.4 V to 0 V vs. RHE with potential interval as 0.1 V.

### 1.8. Product quantification

The yielded  $\text{H}_2\text{O}_2$  was estimated through the  $\text{Ce}(\text{SO}_4)_2$  titration method. After reaction with  $\text{H}_2\text{O}_2$  (equation 4), the  $\text{Ce}^{4+}$  became  $\text{Ce}^{3+}$  in acid media. The linear relation between  $\text{Ce}^{4+}$  and  $\text{H}_2\text{O}_2$  were concluded in equation 5:



$$c_{\text{H}_2\text{O}_2} = 0.5\Delta c_{\text{Ce}^{4+}} \quad (5)$$

UV-Vis spectroscopy was used to detect the  $\text{Ce}^{4+}$  concentration and the linear correlation between  $\text{Ce}^{4+}$  concentration and its absorbance peak was established (Figure S7).  $\text{H}_2\text{O}_2$  yield in the electrolyte can therefore be calculated from the change in  $\text{Ce}^{4+}$  concentration after reaction with the aliquots of electrolyte obtained at a given time.

The faradaic efficiency of the  $\text{H}_2\text{O}_2$  yield ( $FE_{\text{H}_2\text{O}_2}$ ) was determined by the following equation,

$$FE_{\text{H}_2\text{O}_2}(\%) = \frac{2FcV}{Q} \quad (6)$$

Where  $c$  represents the yielded  $\text{H}_2\text{O}_2$  concentration ( $\text{mol L}^{-1}$ ),  $F$  is the faraday constant ( $96485 \text{ C mol}^{-1}$ ),  $V$  indicates the electrolyte volume (L),  $Q$  refers to the consumed charge amount (C).

The cyclohexanone and  $\epsilon$ -caprolactone were quantified by  $^1\text{H}$  NMR (Bruker Avance II 500 MHz) using dimethyl sulfoxide as an internal standard. The conversion of cyclohexanone, faradaic efficiency, yield and selectivity of  $\epsilon$ -caprolactone were calculated according to the following equations:

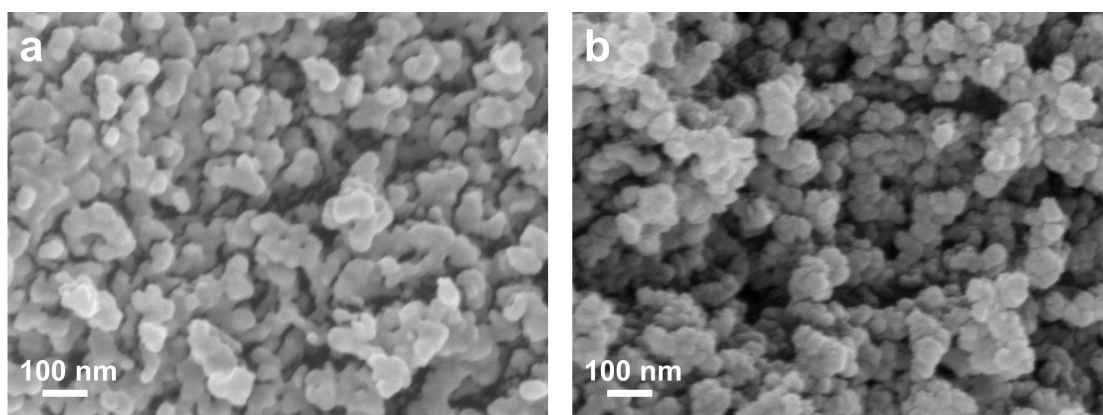
$$\text{Conversion of cyclohexanone (\%)} = \frac{n(\text{initial cyclohexanone}) - n(\text{remaining cyclohexanone})}{n(\text{initial cyclohexanone})} \times 100\% \quad (7)$$

$$\text{Yield (\%)} = \frac{n(\epsilon\text{-caprolactone})}{n(\text{initial cyclohexanone})} \times 100\% \quad (8)$$

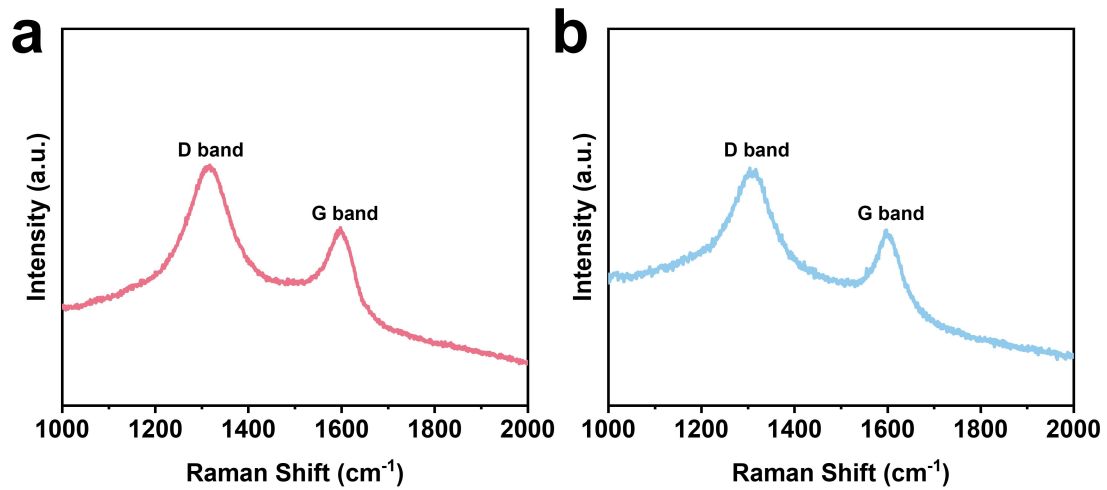
$$FE_{\epsilon\text{-caprolactone}} (\%) = \frac{n(\epsilon\text{-caprolactone}) \times 2 \times 96485}{\text{total consumed charge}} \times 100\% \quad (9)$$

$$\text{Selectivity (\%)} = \frac{\text{Yield}}{\text{Conversion}} \times 100\% \quad (10)$$

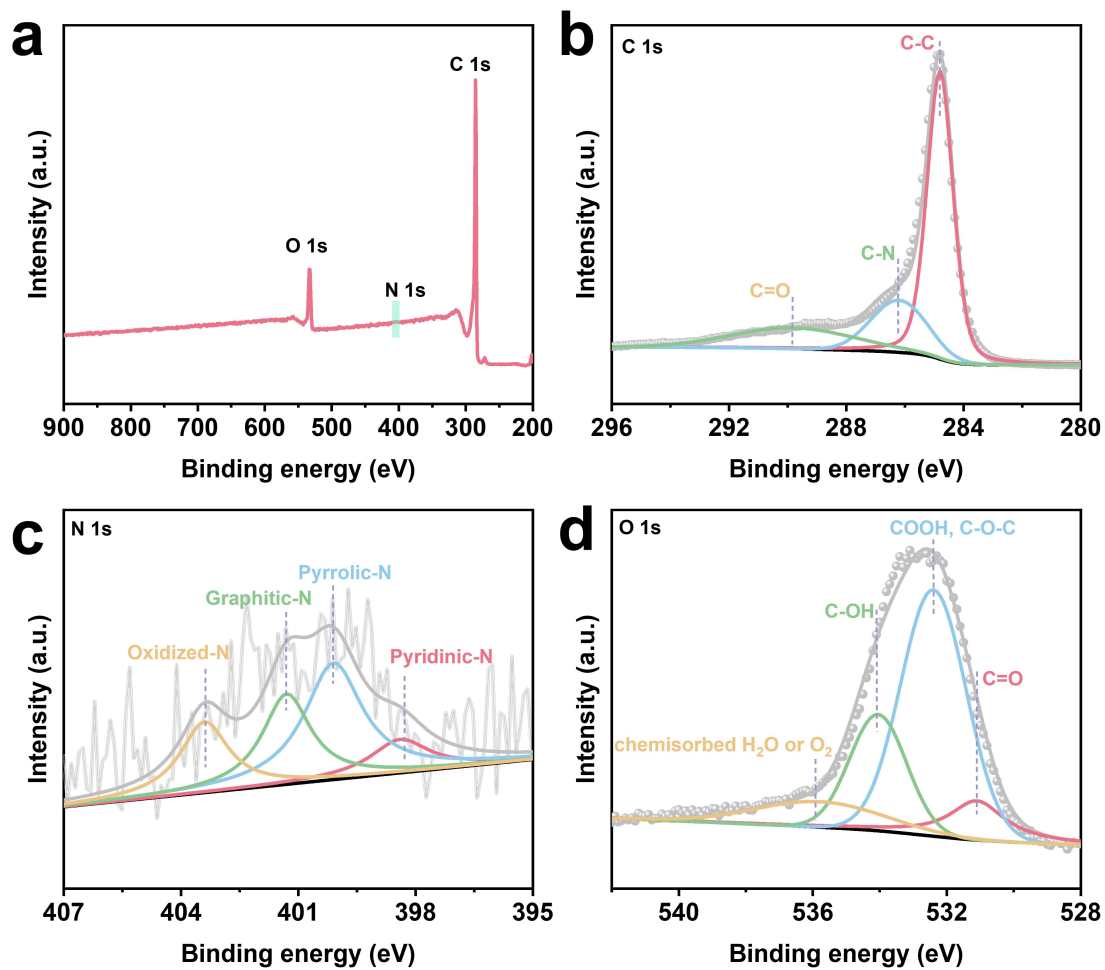
Where  $n(\text{remaining cyclohexanone})$ ,  $n(\text{initial cyclohexanone})$  and  $n(\epsilon\text{-caprolactone})$  are the mole of remaining cyclohexanone after reaction, initial cyclohexanone and generated  $\epsilon$ -caprolactone, respectively.



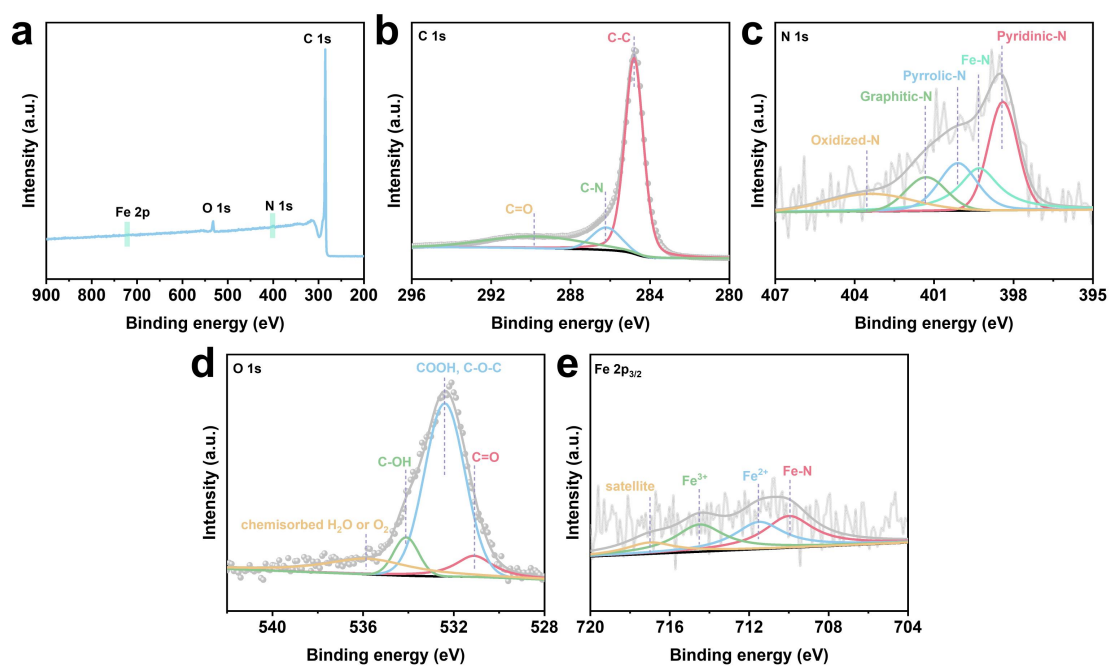
**Figure S1.** SEM images of (a) O@C and (b) Fe<sub>1</sub>NC.



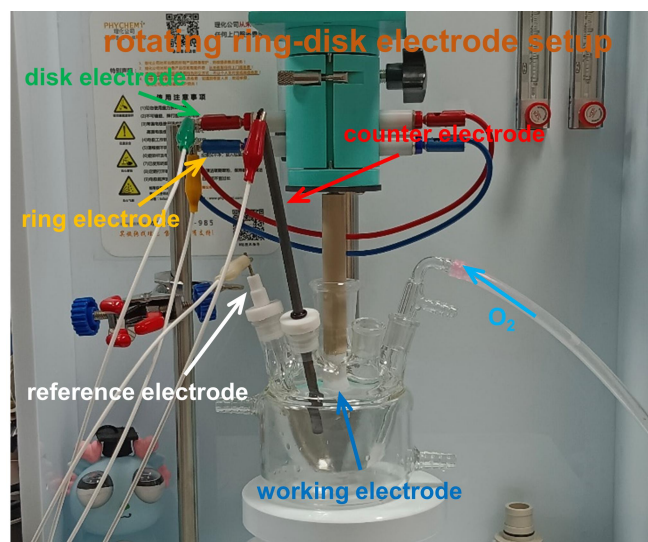
**Figure S2.** Raman spectra of (a) O@C and (b) Fe<sub>1</sub>NC.



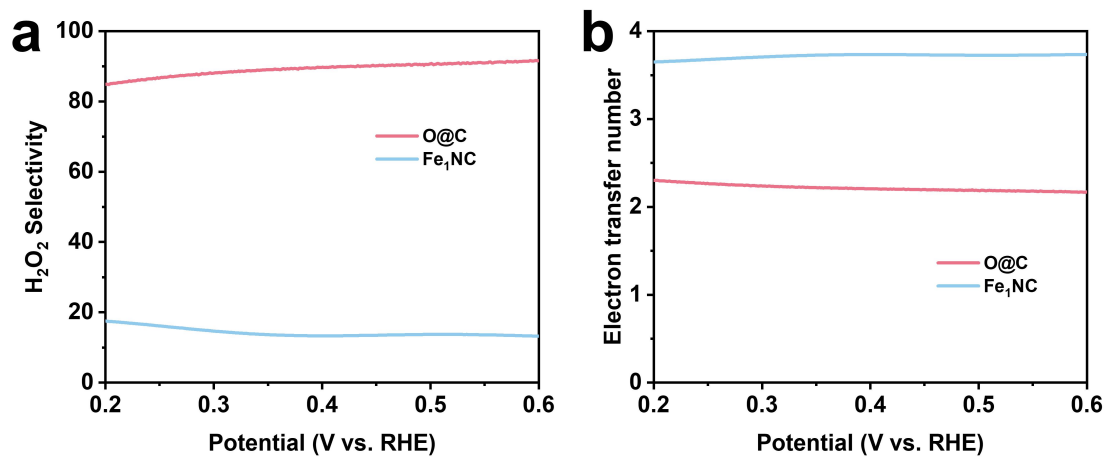
**Figure S3.** (a) XPS survey spectrum, (b) C 1s XPS spectrum, (c) N 1s XPS spectrum, and (d) O 1s XPS spectrum of O@C.



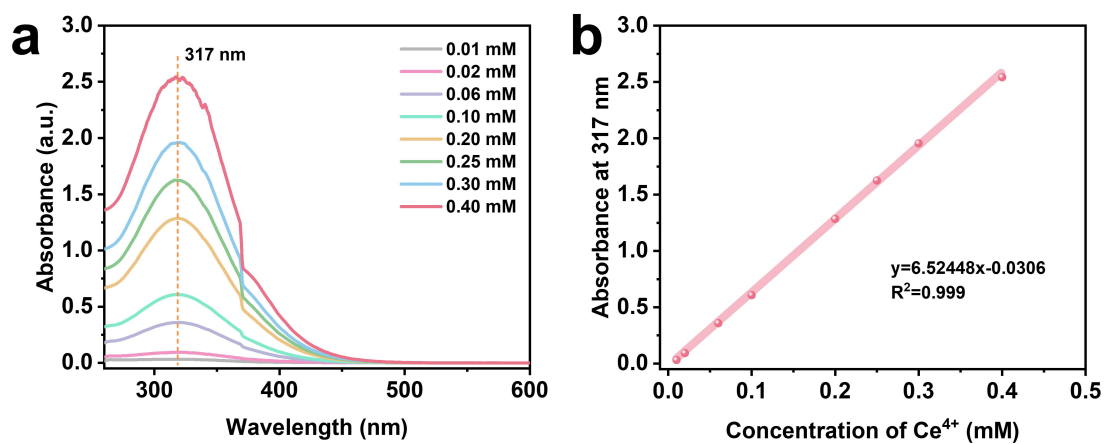
**Figure S4.** (a) XPS survey spectrum, (b) C 1s XPS spectrum, (c) N 1s XPS spectrum, (d) O 1s XPS spectrum, and (e) Fe 2p<sub>3/2</sub> XPS spectrum of Fe<sub>1</sub>NC.



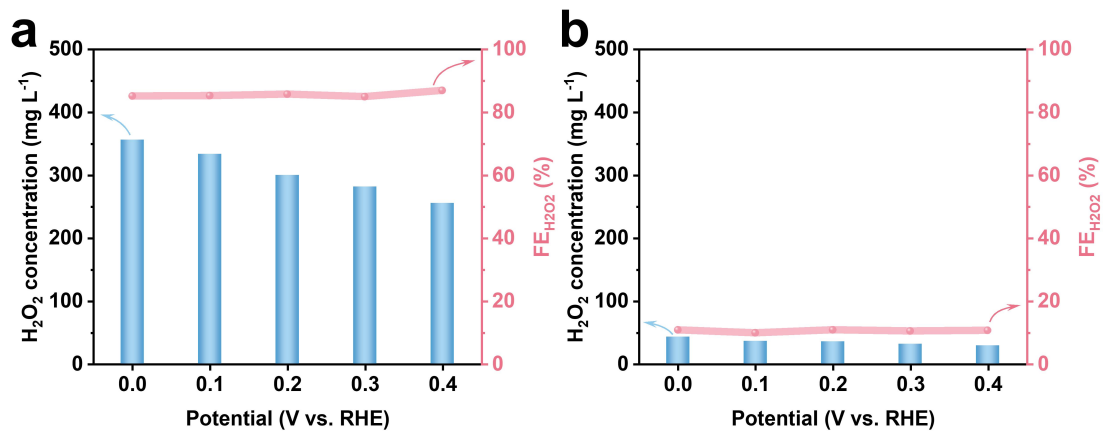
**Figure S5.** Image of used rotating ring-disk electrode setup for 2e<sup>-</sup> ORR test.



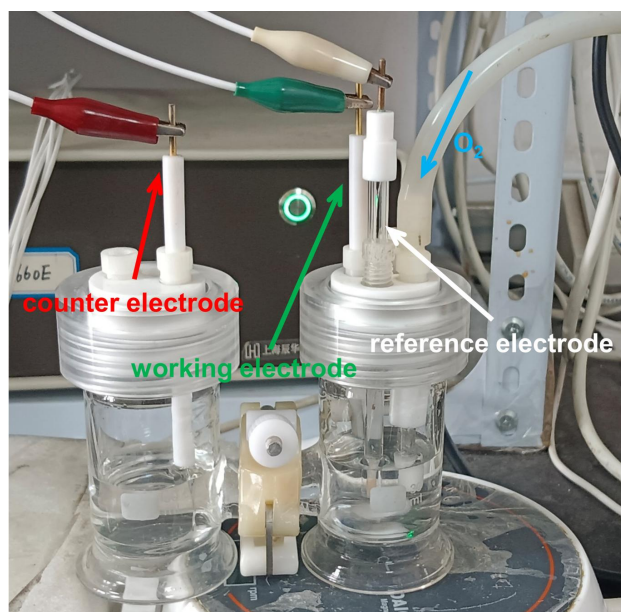
**Figure S6.** (a) H<sub>2</sub>O<sub>2</sub> selectivity and (b) electron transfer number for O@C and Fe<sub>1</sub>NC.



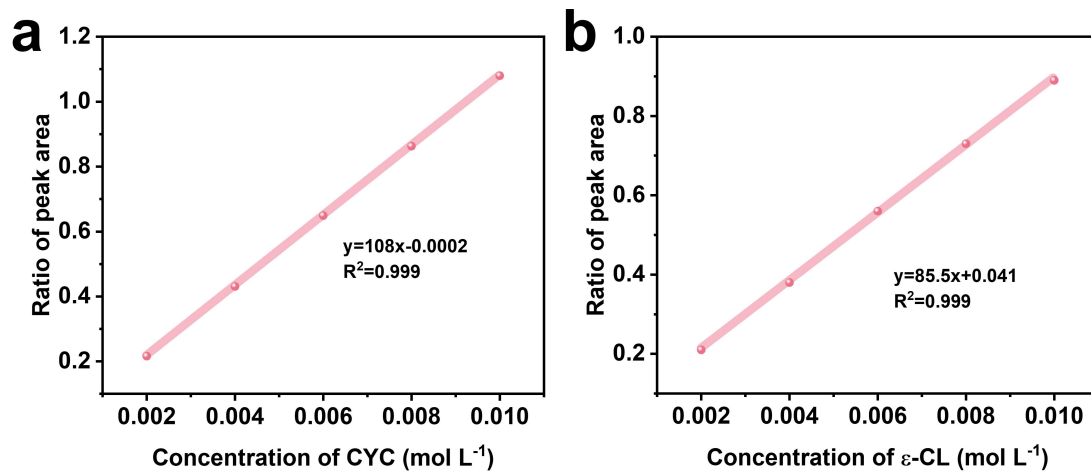
**Figure S7.** (a) UV-vis spectra of  $\text{Ce}^{4+}$  solutions at different concentrations. (b)  $\text{Ce}^{4+}$  absorbance peak at 317 nm against different  $\text{Ce}^{4+}$  concentrations.



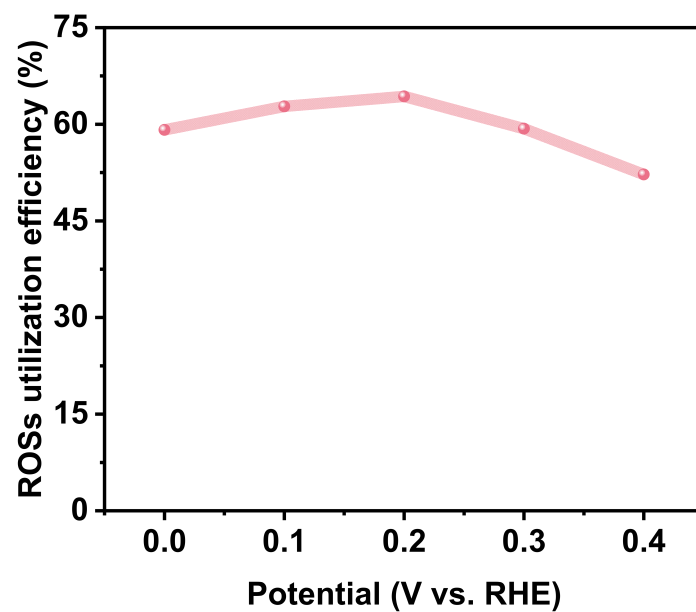
**Figure S8.** H<sub>2</sub>O<sub>2</sub> concentration and Faraday efficiency after electrolysis for 1 h over (a) O@C and (b) Fe<sub>1</sub>NC at different potentials.



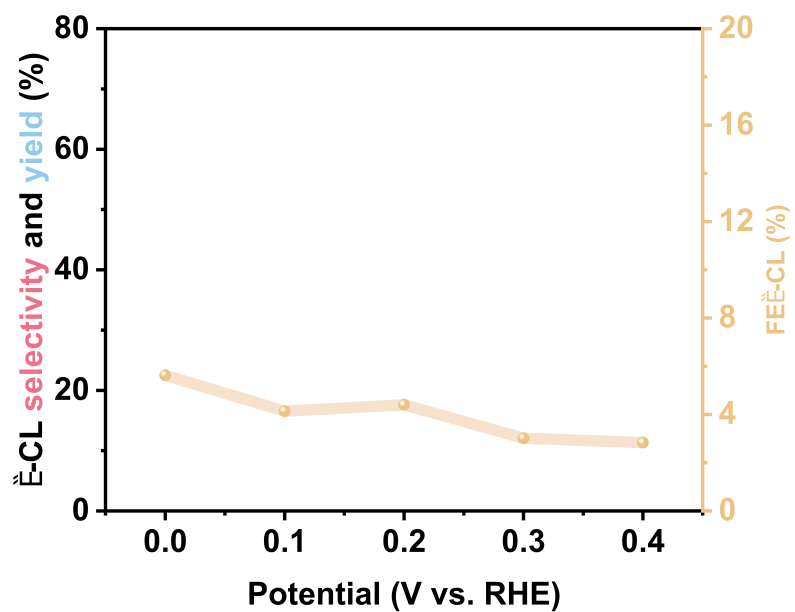
**Figure S9.** H-type electrolytic cell used in the electro-thermochemical cascade reaction



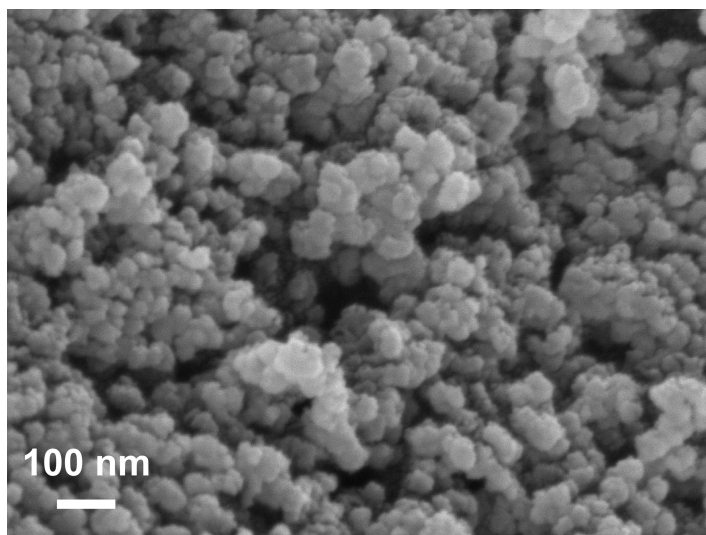
**Figure S10.** The linear relationship between the concentrations of (a) CYC and (b)  $\epsilon$ -CL and the peak areas obtained from the <sup>1</sup>H NMR spectra.



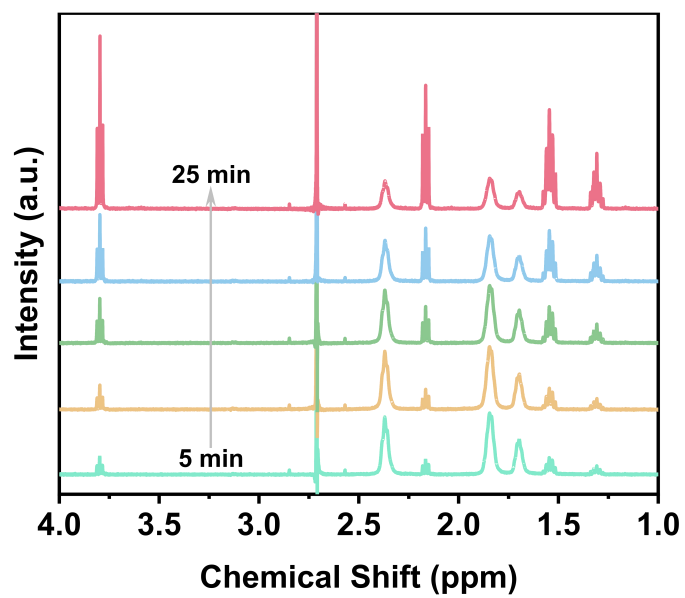
**Figure S11.** The ROSs utilization efficiency for  $\epsilon$ -CL synthesis on O@C in the electro-thermochemical cascade reaction system.



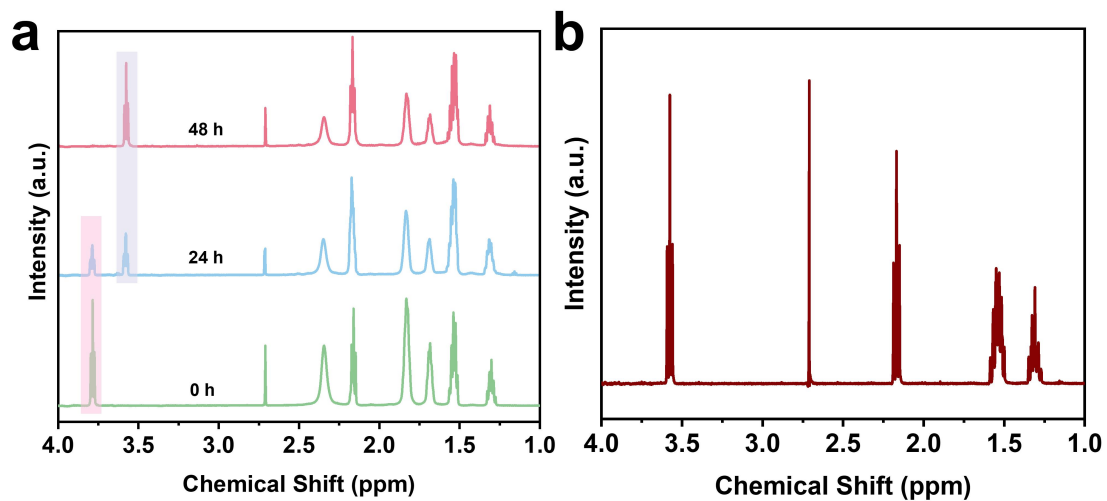
**Figure S12.** Selectivity, yield and Faraday efficiency of  $\epsilon$ -CL obtained by Fe<sub>1</sub>NC within the potential range of 0.4 to 0 V vs. RHE for 1 h electrolysis.



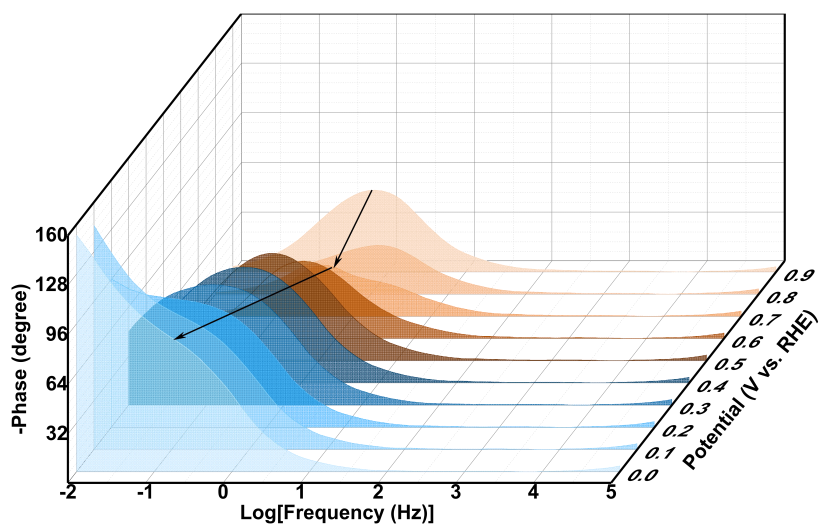
**Figure S13.** SEM image of O@C after reaction.



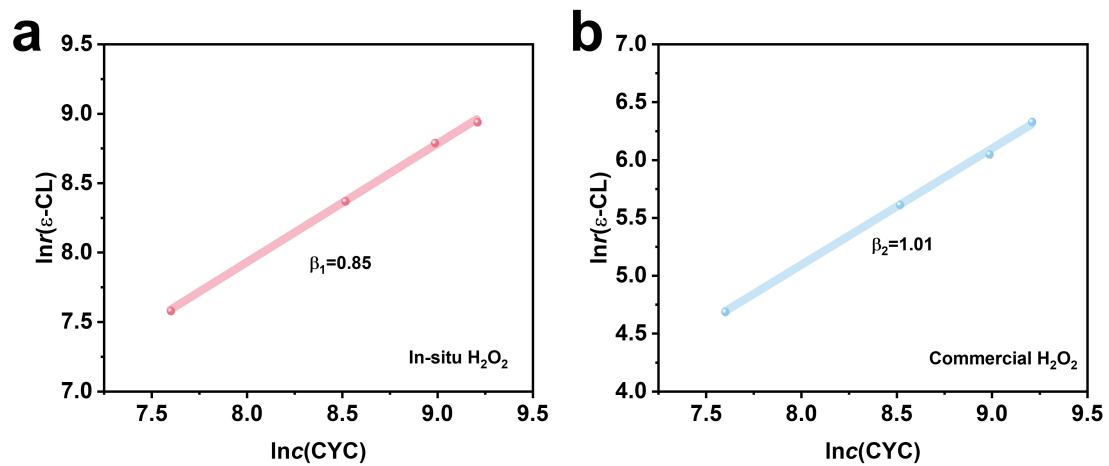
**Figure S14.**  $^1\text{H}$  NMR spectra of the catholyte sampled at regular intervals during the reaction.



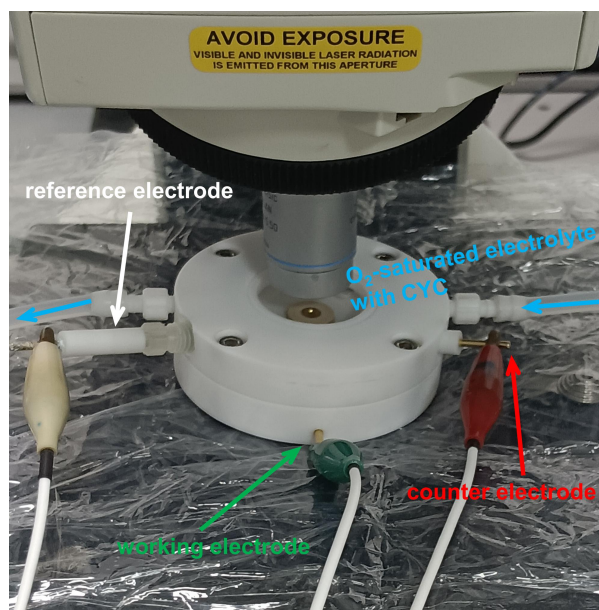
**Figure S15.** (a)  $^1\text{H}$  NMR spectra of the catholyte at 0 h, 24 h, and 48 h post-reaction and (b) 6-hydroxyhexanoic acid standard.



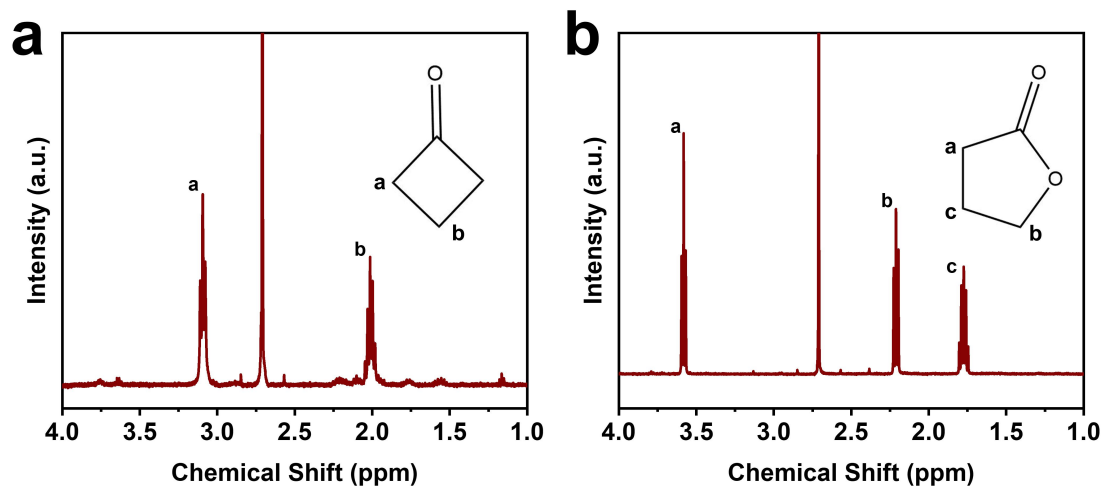
**Figure S16.** Potential-dependent Bode phase plots over Fe<sub>1</sub>NC with CYC in the O<sub>2</sub>-saturated condition.



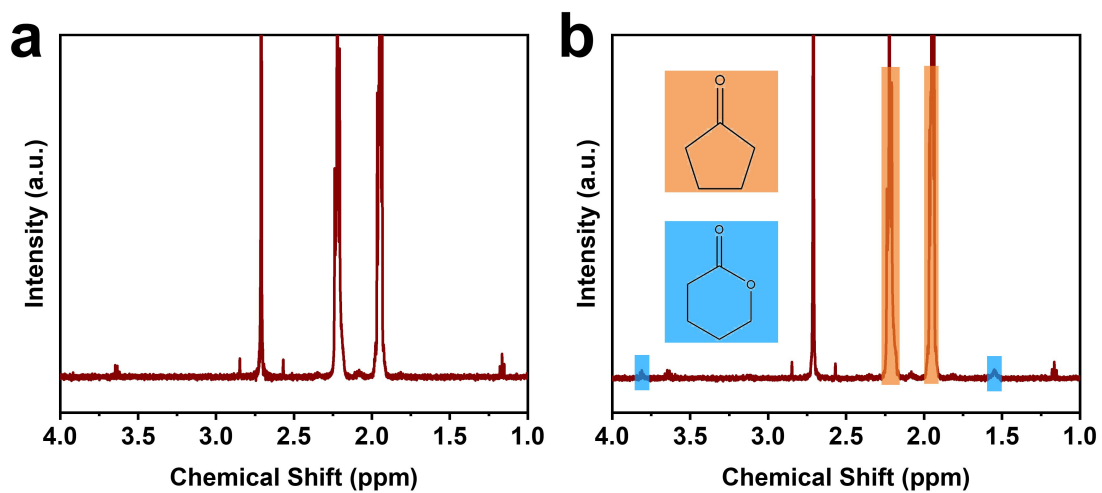
**Figure S17.** Reaction orders of CYC in the (a) in-situ  $2e^-$  ORR-mediated system and (b) commercial  $\text{H}_2\text{O}_2$  system.



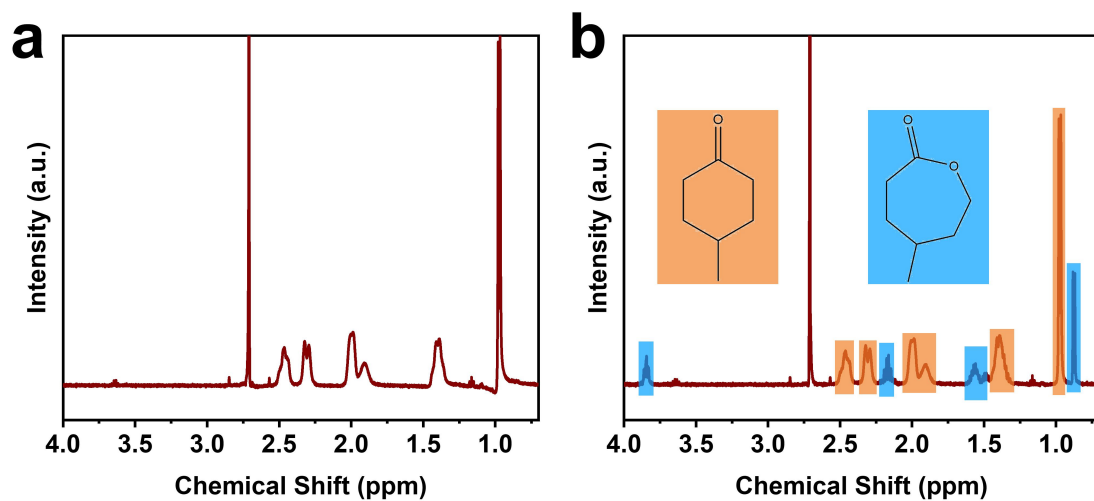
**Figure S18.** Image of used in situ Raman setup.



**Figure S19.** The  $^1\text{H}$  NMR spectra of (a) the electrolyte containing cyclobutanone before the ORR-mediated electro-thermochemical cascade reaction and (b) the electrolyte after the reaction



**Figure S20.** The <sup>1</sup>H NMR spectra of (a) the electrolyte containing cyclopentanone before the ORR-mediated electro-thermochemical cascade reaction and (b) the electrolyte after the reaction.

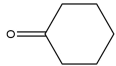
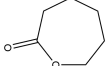
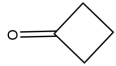
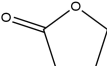
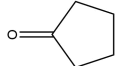
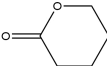


**Figure S21.** The  $^1\text{H}$  NMR spectra of (a) the electrolyte containing 4-methylcyclohexanone before the ORR-mediated electro-thermochemical cascade reaction and (b) the electrolyte after the reaction.

**Table S1.** The comparison of electro-thermochemical cascade catalysis pathway with other available electrochemical synthesis methods.

Method	$\epsilon$ -CL Productivity ( $\mu\text{mol cm}^{-2} \text{h}^{-1}$ )	$\text{FE}_{\epsilon\text{-CL}}$ (%)	Reference
ORR-mediated $\epsilon$ -CL oxidation	180.3	60.1	[1]
Co-oxidation of $\epsilon$ -CL and $\text{H}_2\text{O}_2$	68.4	36.67	[2]
Co-oxidation of $\epsilon$ -CL and $\text{H}_2\text{O}$	26	28.34	[3]
ORR-mediated $\epsilon$ -CL oxidation	198.55	51.4	This work

**Table S2.** Electro-thermochemical cascade catalytic products and corresponding yields and selectivity of various substrates.

Entry	Substrate	Product	Yield (%)	Selectivity (%)
1			79.42	87.54
2			100	100
3			8.43	43.68
4			21.78	79.49

Electrolytic condition: 25 mL electrolyte + 0.01 M substrate + O<sub>2</sub>, O@C as the catalyst, and a constant potential of 0 V vs. RHE for 1 h.

## Reference

- [1] S. Cha, Y. Yang, W. Du, T. Jiang, R. Wang, M. Qu, Z. Ji, C. Yan, X. Yang, and M. Gong, *Angew. Chem. Int. Ed.*, **2025**, e202500546.
- [2] S. Cha, Y. Chen, W. Du, J. Wu, R. Wang, T. Jiang, X. Yang, C. Lian, H. Liu, and M. Gong, *JACS Au*, **2024**, 4, 3629-3640.
- [3] Y. Mu, B. Chen, H. Zhang, M. Fei, T. Liu, N. Mehta, D. Z. Wang, A. J. M. Miller, P. L. Diaconescu, and D. Wang, *J. Am. Chem. Soc.* **2024**, 146, 13438-13444.